JOURNAL OF
EMERGING INVESTIGATORS

Article

Investigating the effects of mutations of amino acids on the protein expression of CDK2 cancer gene

Yash Bhavsar[1], Yajamana Ramu[2]
[1] Moorestown High School, Moorestown, NJ
[2] YARD Sciences, Mount Laurel, NJ

SUMMARY

Each year, twenty million people are diagnosed with cancer. Its prevalence is increasing at a faster pace than any other disease. Cyclin-Dependent Kinase 2 (CDK2) plays a key role in regulating the cell cycle. When CDK2 is overexpressed, it disrupts the cell cycle by accelerating transitions and bypassing checkpoints, leading to uncontrolled cell growth, which is characterized as a hallmark of cancer. There are two approaches to address CDK2 overexpression: one option entails creating mutations in the CDK2 gene that immobilizes its functionality, effectively stopping the cell from dividing and keeping it in a resting phase (G_0 phase). The alternative option is to use CDK2 inhibitors that neutralize its activity. We hypothesized that creating mutations in CDK2 gene's crucial amino acids would lead to significant changes in protein production. We selected seven strategic mutations in two essential regions: the glycine-rich loop and the activation loop. Mutation E12R, located in the glycine-rich loop, inhibited CDK2 gene expression by 80% compared to wild type, while mutation T160E-E162T, located in the activation loop, showed 95% inhibition. Mutation T160L, located in the activation loop, exhibited protein expression levels similar to wild type, whereas mutation T160E, located in the activation loop, resulted in a four-fold increase in CDK2 protein content. The results show that mutations E12R and T160E-E162T were most effective at suppressing CDK2 protein concentration; however, mutation T160E had an opposite effect, leading to increased CDK2 protein concentration. These findings highlight the importance of crucial amino acids in CDK2 expression and their impact on cell growth.

INTRODUCTION

Cancer is one of the most devastating diseases of the 21st century, with more than ten million people losing their lives to cancer each year (1). There has been an increase in newly diagnosed cases by over 26% and deaths by nearly 21% between 2010 and 2019 (2). Cancer is caused by various mutations in the DNA, leading to uncontrolled cell proliferation (3). The cell cycle plays a key role in regulating cell growth, and aberrations in its regulatory components are known to greatly increase the risk of developing cancer (4). The different phases of the cell cycle include G_1 (cell growth), S (DNA replication), G_2 (preparation for division), and mitosis (cell division) (**Figure 1**) (5). Different checkpoints between phases of the cell cycle can detect and correct mutations before the cell transitions to the next phase (6). In instances where these checkpoints detect damage and remain functional, they can halt the cell cycle to allow for repair or push the cell into dormancy or apoptosis if repair is unsuccessful (5-7). However, if the checkpoints themselves are impaired, for example, due to mutations in key regulatory genes, the cell may bypass these safeguards entirely (6). When this happens, damaged cells can proceed unchecked through the cycle, allowing mutations to persist through mitosis and resulting in uncontrolled cell proliferation (8). Many of the most common mutations associated with cancer occur in genes that regulate the cell cycle (9).

Cyclin-dependent kinases (CDKs) are a complex family of serine/threonine kinases that play an essential role in controlling the cell cycle (10). They function by binding to regulatory proteins called cyclins, whose concentrations fluctuate throughout the cell cycle (10). When a CDK binds to its corresponding cyclin, the complex becomes activated and is capable of phosphorylating a variety of substrates that are essential for advancing the cell through specific checkpoints and transitions (10). CDK2 is a 298 amino acid checkpoint gene and its overexpression has been linked to various types of cancers, including lung and breast cancer (11-12). CDK2 consists of two lobes, a carboxy terminus full of alpha helices and an amino terminus with many beta sheets. Between these two lobes is an active site where CDKs bind with cyclins (**Figure 2**) (13). The activation loop and glycine-rich loop of CDK2 are crucial for its activation and binding to cyclins. The

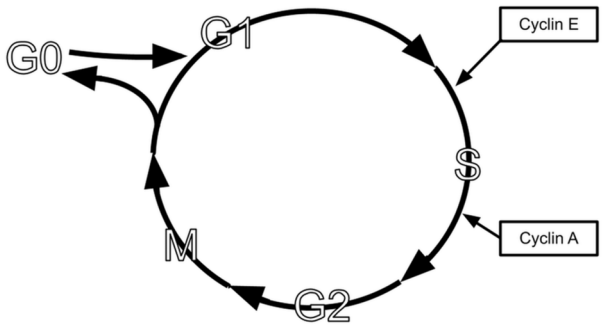

Figure 1: Phases of the cell cycle with cyclin binding sites. The phases shown are: G0 (resting phase), Growth 1 (cell growth and DNA preparation), Synthesis (DNA replication), Growth 2 (organelle duplication and preparation for mitosis), and Mitosis (cell divides). In the G1-S transition, Cyclin E binds with CDK2. Aiding in the end of the S phase, going into the G2 phase, Cyclin A binds with CDK2.

https://doi.org/10.59720/24-290

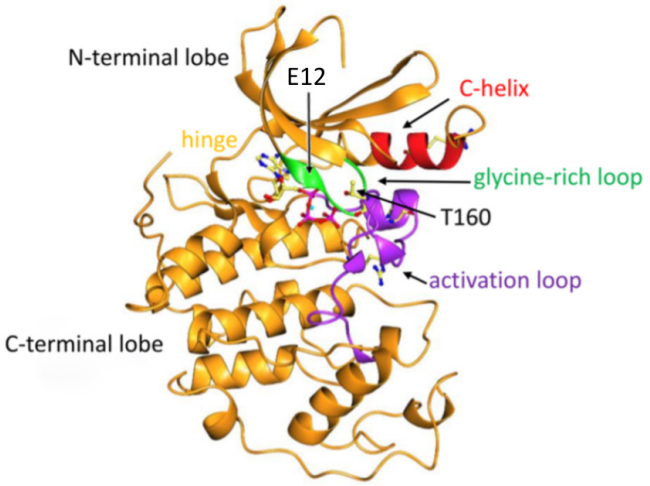

Figure 2: Illustration of Structure of CDK2 Protein (Accession #P24941). The labeled parts include: C-Helix (aids ATP binding and kinase activation), Hinge (anchors ATP), activation loop (regulates substrate binding), glycine-rich loop (coordinates ATP binding and stabilizes active conformation of CDK2), T160 (key phosphorylation site that activates the kinase), and E12 (structure and stability of the protein).

activation loop undergoes phosphorylation after CDK2 binds to cyclin, which stabilizes CDK2 in an active conformation. This phosphorylation induces a structural change that exposes the active site for substrate interaction (13). For example, CDK2 binds with cyclin E and phosphorylates the retinoblastoma protein, leading to the release of transcription factors that activate genes necessary for S phase entry (14). In many cancers, overactivation of this pathway promotes uncontrolled cell proliferation (14). The glycine-rich loop, on the other hand, stabilizes adenosine triphosphate (ATP) binding, which is necessary for the kinase activity of CDK2. Kinase activity refers to CDK2's ability to transfer a phosphate group from ATP to specific substrate proteins. This substrate phosphorylation is essential because it helps regulate DNA replication and cell cycle checkpoints, allowing the cell cycle to progress (15). Together, these structural features enable CDK2 to effectively bind cyclins and perform its role in cell cycle regulation (**Figure 1**) (16-17).

CDK2 binds to two cyclins in cells, Cyclin E and Cyclin A (18-19). Cyclin E binding with CDK2 transitions cells into the S phase, initiating DNA synthesis, whereas Cyclin A binding with CDK2 drives the S phase and G_2/M transition to support DNA synthesis (18-19). This precise regulation ensures orderly cell growth and division (20-21). Through interactions with these cyclins, CDK2 also enforces key checkpoints in the S phase, identifying and correcting any DNA errors (22). However, some mutations can bypass the intra-S phase checkpoint, going unnoticed and surpassing subsequent checkpoints, allowing the cells to grow rapidly (23-26). Overexpression of CDK2 can also contribute to the increased rate of cell growth (27). This can disrupt the normal functionality of checkpoints, contributing to unregulated cell division. This is one of the mechanisms by which CDK2 overexpression can lead to cancer development (28).

One of the approaches to address CDK2 overexpression is to utilize CDK2 inhibitors that neutralize its activity (29). Palbociclib is an FDA-approved CDK inhibitor used to treat breast cancer that prevents CDK4/6 from activation and phosphorylation (30). However, no CDK2 inhibitors have received FDA approval due to increased toxicity and the lack of selectivity (31). This highlights the challenges associated with the development of CDK2 inhibitors as a viable therapeutic strategy. The other approach entails creating targeted mutations in the CDK2 gene that will compromise its functionality, leading to cell cycle arrest (32). The difference between these two approaches is that one inhibits the activation of CDK and the other alters the structure of CDK, both leading to similar results.

We hypothesized that substituting amino acids with different charges and polarities would have a significant impact on protein production. We chose to make mutations in the glycine-rich loop and activation loop because these are two crucial regions that aid in the binding of the cyclin and CDK2. Mutations in these regions could potentially impact CDK2's ability to bind with cyclins, reducing its role in the cell cycle. To achieve this goal, we selected seven strategic mutations and measured their effects on protein production. Our results show that while some mutations significantly increased CDK2 protein content, others reduced protein content.

RESULTS

To test if altering the DNA sequences of crucial amino acids located in the glycine-rich loop and the activation loop of the *CDK2* gene would alter CDK2 expression, we created a total of seven mutations. We created two mutations in the glycine-rich loop (E12R and G13W) and five in the activation loop (T160E, T160Y, T160L, T160E-E162T, and T160E-H161W-E162T) to investigate how structural disruptions affect CDK2 protein content. These mutations were selected based on their potential to alter local charge, size, and polarity. For example, E12 (a negatively charged glutamate) was replaced with R (a positively charged arginine), a change likely to disrupt the glycine-rich loop's flexibility (33). Similarly, T160 (a polar, hydrophilic threonine), an amino acid critical for CDK2 activation, was replaced with residues like glutamate (negatively charged) and leucine (hydrophobic). Combined mutations, such as T160E-E162T and T160E-H161W-E162T, were designed to create even further disruptions and explore crosslinking and interdependencies. These mutations may interfere with local intramolecular interactions, also called crosslinking, by altering various amino acid properties. Such changes can further impact amino acid interdependencies where the structure and behavior of one residue influence neighboring ones (34).

In order to accomplish our objective of creating mutations, we extracted human *CDK2* DNA from plasmids using spin columns and introduced the desired mutation via site-directed mutagenesis. We transformed and plated mutant DNA using *Escherichia coli* (*E. coli*), which was sent for Sanger sequencing to confirm the presence of the correct mutation in the DNA before starting protein production (**Figures 3 and 4**).

	Mean	Standard Deviation	Standard Error
WT (Wild Type)	0.563	0.046	0.023
E12R	0.105	0.024	0.012
T160E	2.175	0.222	0.111
T160L	0.585	0.052	0.026
T160E-E162T	0.036	0.021	0.010

Table 1: Descriptive statistics for OD measurements for WT, E12R, T160E, T160L, T160-E162T at 280nm (n = 4).

https://doi.org/10.59720/24-290

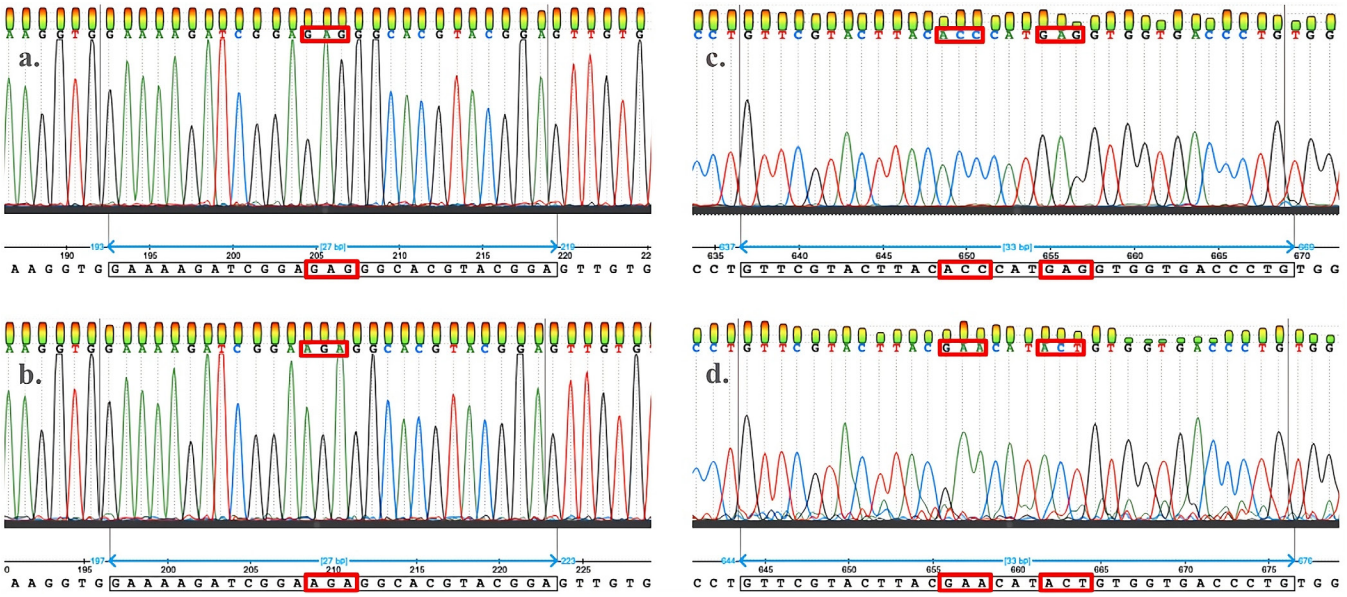

Figure 3: Sanger Sequencing results of E12R and T160E-E162T mutant DNA. Mutant DNA was extracted from colonies and sent to Azenta to perform sanger sequencing. Figures 3a-3d show the results of sanger sequencing performed on both WT and the mutant DNA to confirm that the correct mutation was present. a) Sequence of the WT DNA in glycine-rich loop with trinucleotide sequence encoding glutamic acid (E) boxed in red. b) Sequence of the E12R mutation DNA in glycine-rich loop with trinucleotide sequence encoding arginine (R) boxed in red. c) Sequence of the WT DNA in activation loop with trinucleotide sequences encoding threonine (T) and glutamic acid (E) boxed in red. d) Sequence of the T160E-E162T mutation DNA in activation loop with trinucleotide sequences encoding glutamic acid (E) and threonine (T) boxed in red.

By comparing the DNA sequences of wild-type (WT) and the corresponding mutation, we identified the change of the trinucleotide sequence encoding the mutated amino acid, confirming the success of the mutation (**Figure 3**). We transformed the mutant DNA into *E. coli* (T7 SHuffle) cells for protein production. We lysed these cells and measured the optical density (OD) of the purified protein using a spectrophotometer (**Table 1**).

We converted OD measurements to mass using Beer-Lambert's Law. The WT CDK2 protein yielded 1.55 ± 0.13 mg, which served as the baseline for comparison. Among the glycine-rich loop mutants, E12R resulted in a significant reduction in protein content, approximately 80 percent lower than WT with a protein content of 0.29 ± 0.07 mg ($p < 0.05$), indicating that substituting a negatively charged glutamate with a positively charged arginine may have decreased protein expression. In contrast, the activation loop mutant T160E produced a four-fold increase in protein content of 5.98 ± 0.61 mg ($p < 0.05$), suggesting that mimicking the negative charge added during phosphorylation may enhance expression. T160L, which replaces threonine with a hydrophobic leucine, had protein levels similar to wild-type at 1.61 ± 0.14 mg ($p > 0.05$). Combination of two mutations, T160E-E162T, was created in the activation loop to determine the effects of coupling and interaction on protein expression. Double mutant T160E-E162T led to a 95 percent reduction ($p < 0.05$) in protein yield, dropping to 0.10 ± 0.06 mg, suggesting that the combined changes caused significant interference with protein expression (**Figure 5**). We were not able to successfully quantify three of the seven designed mutations (G13W, T160Y, T160E-H161W-E162T), as all three did not properly amplify during the PCR phase.

In summary, a one-way ANOVA with post hoc Tukey's HSD (honestly significant difference) test revealed that protein content was significantly different in E12R, T160E and T160E-E162T compared to WT ($p < 0.05$). E12R and T160E-E162T exhibited significantly reduced protein content, while T160E showed a significant increase. However, T160L did not show a significant difference compared to WT ($p > 0.05$) (**Figure 5**).

DISCUSSION

Our results show that mutations E12R and T160E-E162T significantly decreased CDK2 protein content compared to WT. They were effective at suppressing CDK2 expression, potentially leading to inhibition of uncontrolled cell growth. On the other hand, mutation T160E substantially increased CDK2 protein content, possibly contributing to increased cell growth. This data confirms our hypothesis that substituting amino acids with different charges and polarity would have a significant impact on CDK2 protein production.

T160 is an essential amino acid for CDK2 functionality (35). Phosphorylation of T160 directly leads to the activation of CDK2 in the G1 and S phases of the cell cycle (36). Furthermore, T160's interaction with nearby amino acids within the activation loop promotes a conformational shift that is essential for cyclin binding and kinase function (37). E162, an amino acid located within the activation loop of CDK2, plays a critical role in the alignment of the active site for interaction with cyclins and other regulators (38). Mutation T160E led to an increase in CDK2 protein levels. T160E mimics phosphorylation and introduces a negatively charged side chain at that position (39). This negative charge is similar to the one added by a phosphate group during phosphorylation (39). Since T106E mimics phosphorylation, it is possible that this modification affects CDK2 stability or expression (39). On the other hand, mutation T160E-E162T significantly

https://doi.org/10.59720/24-290

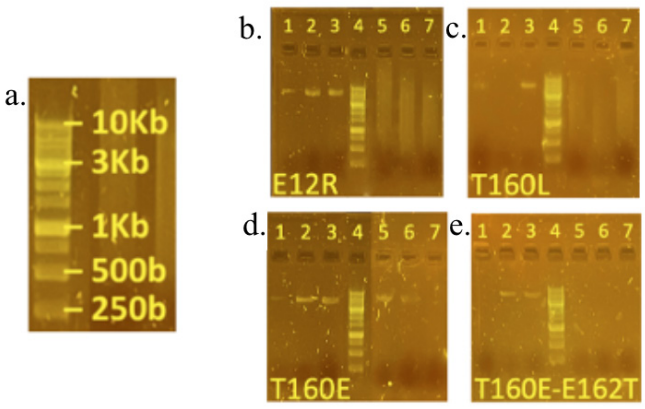

Figure 4: Agarose gel for mutant DNA PCR products. Figure 4a shows an image of the agarose gel and a 1Kb ladder with labeled sizes for base pairs ranging from 10 Kb to 250 b. Figures 4b-4e show the agarose gel electrophoresis that was performed to validate the presence of the gradient PCR products for the mutations E12R, T160L, T160E, and T160E-E162T, respectively. Lanes 1-3 and 5-7 contain gradient PCR products amplified at annealing temperatures of 50°C, 51.6°C, 54.9°C, 58.2°C, 62°C, and 64.4°C, respectively. Lane 4 contains the 1Kb ladder highlighted in 4a.

decreased protein content, demonstrating the importance of crosslinking between T160 and E162 on protein expression. Despite having 298 amino acids, a mutation in just 1 or 2 of the crucial amino acids may lead to changes in protein content.

While the use of CDK2 inhibitors has been explored, no FDA-approved drugs targeting CDK2 inhibition are available, demonstrating its challenges as a viable treatment approach. Our findings suggest that there may be another approach to solving CDK2 overexpression. Our results highlight specific amino acid residues that influence CDK2 protein levels. These sites may serve as potential molecular targets for future therapeutic strategies aimed at modulating CDK2 expression in cancer. However, additional studies are required to elucidate the underlying mechanisms and evaluate their feasibility in a clinical context. Targeting specific mutations within the CDK2 gene can potentially limit toxicities, a common side-effect usually seen with the use of CDK2 inhibitors (40). The benefit of this strategy is controlled regulation of CDK2 overexpression rather than complete inhibition of CDK2 activity.

There are several limitations of our study. Our initial goal was to make seven mutations, but we were only able to complete and find the protein content of four mutations. The main problem was with the binding of the primer to the template DNA during the site-directed mutagenesis. The mutations for which site-directed mutagenesis did not work were G13W, T160Y, and T160E-H161W-E162T. In mutation G13W, we wanted to change from glycine, the smallest amino acid, to tryptophan, the largest amino acid. Mutation T160Y involved a change from threonine, a hydrophilic amino acid, to tyrosine, a very hydrophobic one. Lastly, the triple mutation involved changing multiple amino acids with different properties. In all of these mutations, the primer likely had trouble binding with the DNA template despite the use of different annealing temperatures due to a significant change in nucleotide base pairs in the primers.

Other limitations of this study involve the manner in which the CDK2 protein was isolated and quantified. The CDK2 protein, which contained a His10-TEV tag, was isolated using ZYMOPURE His-Spin Protein MiniPrep. While the use of this technique is accurate in isolating His-tagged proteins, running the obtained sample on an SDS-PAGE gel would have confirmed the sole presence of CDK2 in the purified protein. Since we did not run the sample on an SDS-PAGE gel, it remains possible that trace amounts of other proteins could be present. After obtaining the His-tagged protein, we used ultraviolet-visible (280nm) spectrophotometry as well as the protein's extinction coefficient to determine the concentration of CDK2 in our sample. Using these metrics, protein quantification was calculated. This method has been shown to provide accurate protein quantification, enabling equal protein loading across samples and minimizing variability (41). Alternatively, a Bradford assay could have been used to measure the concentration and quantification of the purified CDK2 protein. Due to experimental constraints, we were unable to perform the Bradford assay.

Our novel findings reveal promise for the future design of CDK2 mutations to regulate its overexpression and impact on uncontrolled cell growth. Future studies should investigate mutations in both the glycine-rich loop and the activation loop simultaneously and measure their effects on the folding of the CDK2 protein. The next steps in carrying our research forward would involve creating similar mutations in a mammalian model and measuring their impact on tumor suppression.

MATERIALS AND METHODS

DNA Extraction

CDK2 slant *Escherichia coli* (DH5-α) cells with bacterial expression and His10-TEV tag, were obtained from AddGene (plasmid #79726) and plated on ampicillin-resistant (100 µg/mL) nutrient agar plates (42). The CDK2 slant was plated in streaked colonies and placed in an incubator at 37°C overnight. The colonies were inoculated into 3mL of ampicillin (100 µg/mL) nutrient broth. This protocol was used for future experiments.

ZymoPURE Plasmid Miniprep Kit (Catalog #D4211) was used to extract plasmid DNA (pDNA) from the CDK2 cell culture. The final step of spin column was transferred to a new microfuge tube, 30µL of ZymoPURE Elution Buffer was added directly to the column matrix, and it was centrifuged at 6000g for 30 seconds. The pDNA was stored at -20°C and was used as needed.

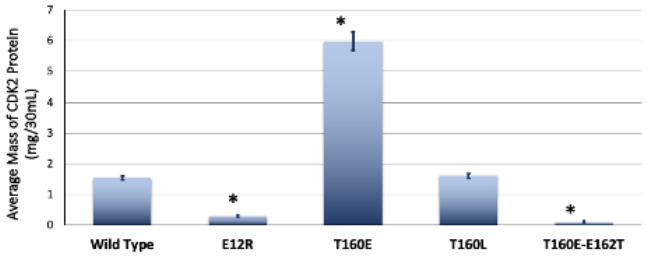

Figure 5: Average mass of protein in milligrams of 30mL *E. coli* culture for WT, E12R, T160E, T160L, T160-E162T (n = 4). Error bars represent standard error of the mean (Equation 1). Asterisks (*) represent statistical significance ($p < 0.05$, one-way ANOVA with post hoc Tukey's HSD Test).

https://doi.org/10.59720/24-290

Gel Electrophoresis

Gel electrophoresis was run using 1% agarose gel to check for the presence of *CDK2* DNA, along with a control 1Kb ladder. 3μL of the DNA, combined with 1μL of 6X Gel Loading Dye, was placed in the well. 5μL of 1Kb ladder was added to the adjacent well to check that the pDNA was the correct size.

Polymerase Chain Reaction (PCR) and Site-Directed Mutagenesis

Seven different mutations were selected within the activation loop and the glycine-rich loop: E12R, G13W, T160E, T160Y, T160L, T160E-E162T, and T160E-H161W-E162T. The forward and reverse desalted primers (**Table 2**) were ordered from GenScript and diluted to 100μM stock. These primers were further made into 2μM stock for site-directed mutagenesis via PCR reaction.

Site-directed mutagenesis was used to generate *CDK2* mutants. It is a technique that is used to create specific, targeted changes in the DNA sequence (43). For each mutation, a 25μL PCR mix consisting of Accuris High Fidelity Master Mix, primers, pDNA, was made according to the manufacturer's directions. To optimize PCR conditions, the mix was further divided into 6 tubes to perform a gradient PCR in order to identify the optimal annealing temperature. Every column had a different annealing temperature, meaning that each mutation had 6 tubes at 6 different temperatures. All tubes were placed in a Thermal Cycler (Benchmark Sci) starting at 95°C for 3 minutes. Sixteen cycles were run to obtain mutated DNA. The cycle included a denaturation phase, an annealing phase, and an extension phase. Gel electrophoresis was conducted to find which annealing temperature was optimal for each mutation (**Figure 4**). Once the correct annealing temperature was identified, a 50 μL standard PCR reaction was performed to attain the mutated DNA via site-directed mutagenesis.

This DNA was then purified using ZymoPURE DNA Clean & Concentrator Kit (Catalog #D4033). To purify the DNA, the manufacturer's instructions were followed. The purified DNA for each mutation was transformed with *E. Coli* (DH5-α) cells and plated on ampicillin-resistant plates. Once the colonies formed, two colonies from each plate were inoculated into nutrient broth with ampicillin. The ZymoPURE Plasmid MiniPrep Kit was used to extract the mutated DNA and it was run on gel electrophoresis to ensure proper size and quality. The DNA samples were then sent for Sanger Sequencing to confirm the presence of the desired mutation.

Name	Sequence
E12R(F)	gaa aag atc gga AGA ggc acg tac gga
E12R(R)	tcc gta cgt gcc TCT tcc gat ctt ttc
T160E(F)	gtt cgt act tac GAA cat gag gtg gtg
T160E(R)	cac cac ctc atg TTC gta agt acg aac
T160L(F)	gtt cgt act tac TTA cat gag gtg gtg
T160L(R)	cac cac ctc atg TAA gta agt acg aac
T160E-E162T(F)	gtt cgt act tac GAA cat ACT gtg gtg acc ctg
T160E-E162T(R)	cag ggt cac cac AGT atg TTC gta agt acg aac

Table 2. Sequences of forward and reverse primers for four successful mutations (E12R, T160E, T160L, & T160E-E162T). Green indicates a mutation in the glycine-rich loop, purple indicates a mutation in the activation loop, and yellow indicates the trinucleotide sequence for the mutated amino acid. The primers were used to create the desired mutations by performing site-directed mutagenesis.

Protein Expression and Purification

After confirming that the sequence had the correct mutation, the DNA was transformed using *E. Coli* (T7 SHuffle) cells onto nutrient agar plates. Half of the colonies from each plate were taken and grown in 30mL nutrient broth solution with ampicillin. Each culture was further divided into two 15mL cultures for centrifugation.

A spectrophotometer (Metash) was used to monitor the OD of each culture at 600nm. Once the OD reached ~0.8, 15 μL of isopropyl β-D-1-thiogalactopyranoside (IPTG 0.5mM) was added to induce protein production and grown overnight. The cells were centrifuged at 4000g for 6 minutes. The supernatant was discarded and the cell pellet was then dislodged using 2mL of Phosphate Buffer Solution with 20μL of 100X Protease Inhibitor Cocktail Mix. This solution was then placed into a 2mL Lysing Matrix tube with silica beads. The MonoLyser was used to lyse the cells and collect the protein. ZYMOPure His-Spin Protein MiniPrep Kit (Catalog #P2002) was used according to the manufacturer's instructions to isolate the protein in the solutions, purifying the His-tagged protein from the cell lysate. Finally, the spectrophotometer was used to take readings of the protein content at 280nm with quartz cuvettes.

Data Analysis

Standard error of mean (SEM) was calculated using standard deviation (σ) and sample size (n) **(Equation 1)**, where σ is the standard deviation and n is the sample size.

$$SEM = \frac{\sigma}{\sqrt{n}}$$

The SEM value is graphed as positive and negative error bars (**Figure 5**).

To calculate the protein content from the OD measurements (**Table 1**), we used the Beer-Lambert Law (**Equation 2**), where A is the absorbance (OD) at 280nm, ε is the extinction coefficient of the protein, c is the concentration of the protein, and l is the path length of the cuvette.

$$A = \varepsilon c l$$

To simplify calculations, this can be rearranged (**Equation 3**).

$$c = \frac{A}{\varepsilon l}$$

By using the observed values of absorbance, an extinction coefficient of 37025 $M^{-1}cm^{-1}$ (44), and a path length of 1, the concentration of the protein can be calculated. This can be converted from moles per liter to grams per liter (**Equation 4**), where g is the concentration of the protein in g/L, c is the concentration of the protein in mol/L, and m is the molar mass.

$$g = c * m$$

Substituting the calculated value for c and a molar mass of 33929.53g/mol (26), the concentration of the protein can be obtained in g/L. Finally, the concentration can be converted to mass (**Equation 5**), where p is the mass of the protein in grams, g is the concentration of protein, v is the volume of the cuvette in liters.

$$p = g * v$$

Substituting the calculated value for g and a volume of 0.003L (3mL), the concentration of the protein can be

https://doi.org/10.59720/24-290

converted to mass in grams, *p*.

To calculate statistical significance between the calculated protein contents of WT and the four mutations (E12R, T160E, T160L, T160-E162T) one way ANOVA was used followed by post hoc Tukey's HSD test. This statistical analysis was performed using Statistical Package for Social Sciences (SPSS, v30).

Received: August 27, 2024
Accepted: March 17, 2025
Published: October 1, 2025

REFERENCES

1. "Cancer Statistics." Cancer.gov, Cancer.gov, 9 May 2024, https://www.cancer.gov/about-cancer/understanding/statistics#:~:text=Cancer%20is%20among%20the%20leading,ranks%20low%20on%20these%20measures
2. Kocarnik, Jonathan M., *et al*. "Cancer Incidence, Mortality, Years of Life Lost, Years Lived with Disability, and Disability-Adjusted Life Years for 29 Cancer Groups from 2010 to 2019." JAMA Oncology, vol. 8, no. 3, American Medical Association (AMA), Mar. 2022, p. 420, https://doi.org/10.1001/jamaoncol.2021.6987
3. Hanahan, Douglas, and Robert A Weinberg. "Hallmarks of Cancer: The next Generation." *Cell*, vol. 144, no. 5, Cell Press, Mar. 2011, pp. 646–74, https://doi.org/10.1016/j.cell.2011.02.013
4. Dai, Yun, *et al*. "Cell Cycle Regulation and Hematologic Malignancies." Blood Science, vol. 1, no. 1, Ovid Technologies (Wolters Kluwer Health), Aug. 2019, pp. 34–43, https://doi.org/10.1097/bs9.0000000000000009
5. Vermeulen, Katrien, *et al*. "The Cell Cycle: A Review of Regulation, Deregulation and Therapeutic Targets in Cancer." *Cell Proliferation*, vol. 36, no. 3, Wiley, June 2003, pp. 131–49, https://doi.org/10.1046/j.1365-2184.2003.00266.x
6. Hartwell, Leland H., and Ted A. Weinert. "Checkpoints: Controls That Ensure the Order of Cell Cycle Events." Science, vol. 246, no. 4930, American Association for the Advancement of Science, Nov. 1989, pp. 629–34, https://doi.org/10.1126/science.2683079
7. Campisi, Judith, and Fabrizio. "Cellular Senescence: When Bad Things Happen to Good Cells." Nature Reviews Molecular Cell Biology, vol. 8, no. 9, Nature Portfolio, Sept. 2007, pp. 729–40, https://doi.org/10.1038/nrm2233
8. Kastan, Michael B., and Jiri Bartek. "Cell-Cycle Checkpoints and Cancer." *Nature*, vol. 432, no. 7015, Nature Portfolio, Nov. 2004, pp. 316–23, https://doi.org/10.1038/nature03097
9. Radoslav Stojchevski, *et al*. "Translational Advances in Oncogene and Tumor-Suppressor Gene Research." Cancers, vol. 17, no. 6, Multidisciplinary Digital Publishing Institute, Mar. 2025, pp. 1008–8, https://doi.org/10.3390/cancers17061008
10. Ilenia Pellarin, *et al*. "Cyclin-Dependent Protein Kinases and Cell Cycle Regulation in Biology and Disease." Signal Transduction and Targeted Therapy, vol. 10, no. 1, Springer Nature, Jan. 2025, https://doi.org/10.1038/s41392-024-02080-z
11. Said Akli, *et al*. "Cdk2 Is Required for Breast Cancer Mediated by the Low-Molecular-Weight Isoform of Cyclin E." Cancer Research, vol. 71, no. 9, American Association for Cancer Research, Apr. 2011, pp. 3377–86, https://doi.org/10.1158/0008-5472.can-10-4086
12. Casado-Vela, Juan, *et al*. "Differential Phosphorylation Patterns between the Cyclin-A2/CDK2 Complex and Their Monomers." Protein Expression and Purification, vol. 66, no. 1, Elsevier BV, July 2009, pp. 15–21, https://doi.org/10.1016/j.pep.2009.02.007
13. Malumbres, Marcos. "Cyclin-Dependent Kinases." Genome Biology, vol. 15, no. 6, Springer Science+Business Media, Jan. 2014, pp. 122–22, https://doi.org/10.1186/gb4184
14. Akiyama, T., *et al*. "Phosphorylation of the Retinoblastoma Protein by Cdk2." Proceedings of the National Academy of Sciences, vol. 89, no. 17, National Academy of Sciences, Sept. 1992, pp. 7900–4, https://doi.org/10.1073/pnas.89.17.7900
15. Iveta Bártová, *et al*. "Functional Flexibility of Human Cyclin-Dependent Kinase-2 and Its Evolutionary Conservation." Protein Science, vol. 17, no. 1, Wiley, Nov. 2007, pp. 22–33, https://doi.org/10.1110/ps.072951208
16. Jeffrey, Philip D., *et al*. "Mechanism of CDK Activation Revealed by the Structure of a CyclinA-CDK2 Complex." *Nature*, vol. 376, no. 6538, Nature Portfolio, July 1995, pp. 313–20, https://doi.org/10.1038/376313a0
17. Brown, Nick R., *et al*. "The Structural Basis for Specificity of Substrate and Recruitment Peptides for Cyclin-Dependent Kinases." Nature Cell Biology, vol. 1, no. 7, Springer Science and Business Media LLC, Oct. 1999, pp. 438–43, https://doi.org/10.1038/15674
18. Fagundes, Rafaela, and Leonardo K. Teixeira. "Cyclin E/CDK2: DNA Replication, Replication Stress and Genomic Instability." Frontiers in Cell and Developmental Biology, vol. 9, Frontiers Media, Nov. 2021, https://doi.org/10.3389/fcell.2021.774845
19. Oakes, Vanessa, *et al*. "Cyclin A/Cdk2 Regulates Cdh1 and Claspin during Late S/G2 Phase of the Cell Cycle." Cell Cycle, vol. 13, no. 20, Informa UK Limited, Oct. 2014, pp. 3302–11, https://doi.org/10.4161/15384101.2014.949111
20. Lim, Shuhui, and Philipp Kaldis. "Cdks, Cyclins and CKIs: Roles beyond Cell Cycle Regulation." Development, vol. 140, no. 15, The Company of Biologists, Aug. 2013, pp. 3079–93, https://doi.org/10.1242/dev.091744
21. Wood, Daniel J., and Jane A. Endicott. "Structural Insights into the Functional Diversity of the CDK–Cyclin Family." Open Biology, vol. 8, no. 9, Royal Society, Sept. 2018, https://doi.org/10.1098/rsob.180112
22. Bačević, Katarina, *et al*. "Cdk2 Strengthens the Intra-S Checkpoint and Counteracts Cell Cycle Exit Induced by DNA Damage." Scientific Reports, vol. 7, no. 1, Springer Science and Business Media LLC, Oct. 2017, https://doi.org/10.1038/s41598-017-12868-5
23. Geng, Yan, *et al*. "Kinase-Independent Function of Cyclin E." Molecular Cell, vol. 25, no. 1, Elsevier BV, Jan. 2007, pp. 127–39, https://doi.org/10.1016/j.molcel.2006.11.029
24. Harper, J. W., and P. D. Adams. "Cyclin-Dependent Kinases." Chemical Reviews, vol. 101, no. 8, American Chemical Society, July 2001, pp. 2511–26, https://doi.org/10.1021/cr0001030
25. Johnson, Neil, *et al*. "Cdk1 Participates in BRCA1-Dependent S Phase Checkpoint Control in Response to

https://doi.org/10.59720/24-290

DNA Damage." Molecular Cell, vol. 35, no. 3, Elsevier BV, Aug. 2009, pp. 327–39, https://doi.org/10.1016/j.molcel.2009.06.036
26. Koff, Andrew, *et al*. "Human Cyclin E, a New Cyclin That Interacts with Two Members of the CDC2 Gene Family." Cell, vol. 66, no. 6, Cell Press, Sept. 1991, pp. 1217–28, https://doi.org/10.1016/0092-8674(91)90044-y
27. Tetsu, Osamu, and Frank McCormick. "Proliferation of Cancer Cells despite CDK2 Inhibition." *Cancer Cell*, vol. 3, no. 3, Elsevier BV, Mar. 2003, pp. 233–45, https://doi.org/10.1016/s1535-6108(03)00053-9
28. Pucci, Bruna, *et al*. "Cell Cycle and Apoptosis." *Neoplasia*, vol. 2, no. 4, Elsevier BV, July 2000, pp. 291–99, https://doi.org/10.1038/sj.neo.7900101
29. Whittaker, Steven R., *et al*. "Inhibitors of Cyclin-Dependent Kinases as Cancer Therapeutics." Pharmacology & Therapeutics, vol. 173, Elsevier BV, May 2017, pp. 83–105, https://doi.org/10.1016/j.pharmthera.2017.02.008
30. Turner, Nicholas C., *et al*. "Palbociclib in Hormone-Receptor–Positive Advanced Breast Cancer." New England Journal of Medicine, vol. 373, no. 3, Massachusetts Medical Society, July 2015, pp. 209–19, https://doi.org/10.1056/nejmoa1505270
31. Zeng, Yangjie, *et al*. "Inhibitors and PROTACs of CDK2: Challenges and Opportunities." Expert Opinion on Drug Discovery, vol. 19, no. 9, Informa UK Limited, July 2024, pp. 1125–48, https://doi.org/10.1080/17460441.2024.2376655
32. Long, Xiang-E., *et al*. "Suppression of CDK2 Expression by SiRNA Induces Cell Cycle Arrest and Cell Proliferation Inhibition in Human Cancer Cells." BMB Reports, vol. 43, no. 4, Korean Society for Biochemistry and Molecular Biology - BMB Reports, Apr. 2010, pp. 291–96, https://doi.org/10.5483/bmbrep.2010.43.4.291
33. Bártová, Iveta, *et al*. "Activation and Inhibition of Cyclin-Dependent Kinase-2 by Phosphorylation; a Molecular Dynamics Study Reveals the Functional Importance of the Glycine-Rich Loop." Protein Science, vol. 13, no. 6, Wiley, June 2004, pp. 1449–57, https://doi.org/10.1110/ps.03578504
34. Yang, Bing, *et al*. "Spontaneous and Specific Chemical Cross-Linking in Live Cells to Capture and Identify Protein Interactions." Nature Communications, vol. 8, no. 1, Nature Portfolio, Dec. 2017, https://doi.org/10.1038/s41467-017-02409-z
35. Gu, Y., *et al*. "Cell Cycle Regulation of CDK2 Activity by Phosphorylation of Thr160 and Tyr15." The EMBO Journal, vol. 11, no. 11, Springer Nature, Nov. 1992, pp. 3995–4005, https://doi.org/10.1002/j.1460-2075.1992.tb05493.x
36. Subbareddy Maddika, *et al*. "Akt-Mediated Phosphorylation of CDK2 Regulates Its Dual Role in Cell Cycle Progression and Apoptosis." Journal of Cell Science, vol. 121, no. 7, 19 Mar. 2008, pp. 979–988, https://doi.org/10.1242/jcs.009530
37. Düster, Robert, *et al*. "Structural Basis of Cdk7 Activation by Dual T-Loop Phosphorylation." BioRxiv (Cold Spring Harbor Laboratory), 14 Feb. 2024, https://doi.org/10.1101/2024.02.14.580246
38. Martinez, A. -M . "Dual Phosphorylation of the T-Loop in Cdk7: Its Role in Controlling Cyclin H Binding and CAK Activity." The EMBO Journal, vol. 16, no. 2, Springer Science and Business Media LLC, Jan. 1997, pp. 343–54, https://doi.org/10.1093/emboj/16.2.343
39. Zhang, Jiawei, *et al*. "Inhibition of the CDK2 and Cyclin a Complex Leads to Autophagic Degradation of CDK2 in Cancer Cells." Nature Communications, vol. 13, no. 1, Nature Portfolio, May 2022, https://doi.org/10.1038/s41467-022-30264-0
40. House, Isabelle, *et al*. "Cyclin Dependent Kinase 2 (CDK2) Inhibitors in Oncology Clinical Trials: A Review." Journal of Immunotherapy and Precision Oncology, vol. 8, no. 1, Dec. 2024, pp. 47–54, https://doi.org/10.36401/jipo-24-22
41. Gill, Stanley C., and Peter H. von Hippel. "Calculation of Protein Extinction Coefficients from Amino Acid Sequence Data." Analytical Biochemistry, vol. 182, no. 2, Nov. 1989, pp. 319–326, https://doi.org/10.1016/0003-2697(89)90602-7
42. Albanese, Steven K., *et al*. "An Open Library of Human Kinase Domain Constructs for Automated Bacterial Expression." Biochemistry, vol. 57, no. 31, American Chemical Society, July 2018, pp. 4675–89, https://doi.org/10.1021/acs.biochem.7b01081
43. Bachman, Julia. "Site-Directed Mutagenesis." Methods in Enzymology on CD-ROM/Methods in Enzymology, Academic Press, Jan. 2013, pp. 241–48, https://doi.org/10.1016/b978-0-12-418687-3.00019-7
44. "Expasy - ProtParam." Expasy.org, 2025, https://web.expasy.org/cgi-bin/protparam/protparam_bis.cgi?P24941